Persistent Voltage Control of a Wind Turbine-Driven Isolated Multiphase Induction Machine

Marwa Ben Slimene
College of Computer Science and Engineering, University of Ha'il, Saudi Arabia | SIME Laboratory, ENSIT, University of Tunis, Tunisia
benslimene.marwa@gmail.com (corresponding author)

Mohamed Arbi Khlifi
Department of Electrical Engineering, Islamic University of Madinah, Saudi Arabia | SIME Laboratory, ENSIT, University of Tunis, Tunisia
medarbi.khlifi@gmail.com (corresponding author)

Received: 26 August 2023 | Revised: 11 September 2023 | Accepted: 12 September 2023

 DOI: https://doi.org/10.48084/etasr.6330

ABSTRACT

The growing concern about the energy crisis and environmental protection has caused a growing interest in wind power generation systems. Researchers and engineers urgently need to create new multiphase induction machines for the production of wind energy, since they are essential parts of wind turbines. This study offers control and stability analysis of a multiphase induction machine based on the entropy stability requirements for its linearized model. The generated model was used to assess the on-load properties of the multiphase induction machine and calculate its steady-state parameters under each operating circumstance. According to the analysis, the eigenvalues depend on the machine parameters, with the excitation capacitance and speed variation being the most important. Stabilization of the multiphase induction machine is the main focus of the singular values, which vary according to its variables. The simulated results include an examination of a multiphase induction machine steady state for voltage build-up at various types of load.

Keywords-multi-phase machine; efficiency curves; stability analysis; equivalent circuit; control strategies

I. INTRODUCTION

Research on power transmission has gone beyond three phases [1-2], and multiphase induction machines have become much more significant [3-4]. Multiphase machines are seen as an alternative to three-phase machines for applications that need a range of speeds. As the demand for wind turbines and sustainable mobility increases worldwide, multiphase machines have become one of the preferred options for power conversion systems. Research on multiphase machines is becoming more and more popular due to the development of power semiconductor devices and converter modulation techniques. The stator excitation in a multiphase machine produces improved magneto-motive force, resulting in lower space harmonics, lower torque ripples, and higher efficiency than in three-phase drives. Multiphase drives also offer many other exceptional advantages over traditional three-phase drives [5-6]. Additional phases, strong reliability standards, and higher power ratings provide the system with more room for advancement, making multiphase machines preferable to their three-phase counterparts. As a result, research on multiphase machines has been expanding [7-8]. High-phase machines provide greater operating flexibility and fault tolerance compared to their three-phase counterparts [9-10].

In this study, the multiphase machine under investigation used a single three-phase winding set excitation technique. At least three different loading topologies can be used. For example, a load could be fed by a six-phase transformer that interfaces with the load. Although de-rating of the load is rarely necessary when even two phases are lost, such a configuration produces an exceedingly fault-resilient loading architecture [11-12]. Energy is regularly extracted from many renewable energy sources, such as small hydro plants, wind turbines, etc., using six-phase induction generators, since they have several benefits, including ease of construction, low cost, toughness, high dependability, and low maintenance requirements [13-14]. Multiphase induction generators have many advantages over conventional three-phase systems. Systems with more than three phases have recently attracted a great deal of interest in variable-speed drive electric systems [15-16]. Multiphase machines are used in important applications that demand strong fault-tolerant capabilities, such as submarine propulsion, aircraft, and undoubtedly Electric Vehicles (EVs) [17-20].

The loss of one phase does not cause a breakdown of the spinning magnetic field in three-phase machines without a neutral-point connection. Three phases are the bare minimum that can be used to provide the required rotational field. A multiphase machine can still operate without stopping if one of the phases is open-circuited [21-24]. Multiphase induction generators can easily increase the total amount of power while maintaining the prior per-phase power rating. However, compared to multiphase induction generators, research on multiphase induction motors has been more fruitful to date [25-28]. Due to their higher reliability, multiphase machines are beginning to be accepted as alternatives in high-power applications because of their potential to create fault-tolerant operating procedures. High-power applications also have the advantage of requiring half as much power per phase for any given output power, allowing the use of power semiconductors with lower ratings than three-phase systems [30-34].

This study focuses on the working modes of a multiphase induction machine, determining the static performance of the self-excited generator at no and under load and examining the influence of capacity and speed variation on the electrical quantities. All analytical and numerical simulation studies were validated by experimental tests using a prototype available in the laboratory.

II. MATHEMATICAL MODEL OF MPIM

Figure 1 shows the schematic architecture of a multiphase induction generator for its two different sets of three-phase stator windings and one rotor winding. There is an arbitrary angle that separates these two sets of three-phase stator windings from the stars.

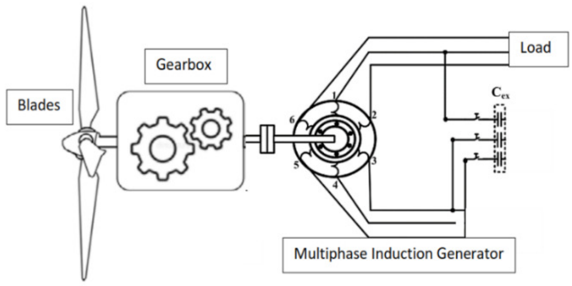

Fig. 1. Configuration of a wind-based MPIM.

Figure 2 shows the *d-q* model applied as the loading is applied.

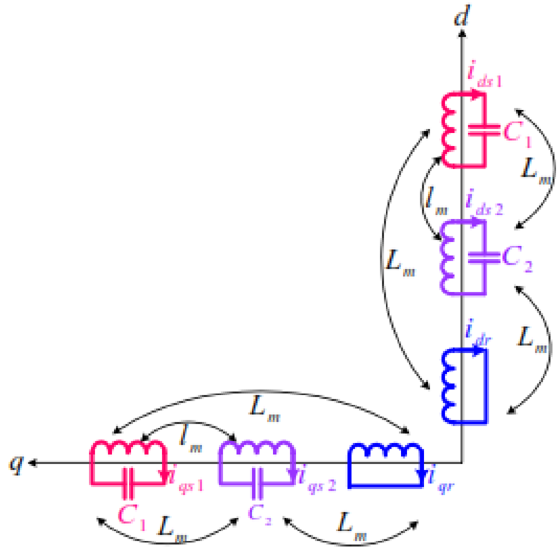

Fig. 2. Park transformation of multi-phase induction generator.

The multi-stator winding induction machine model was developed as follows:

$$[X] = \left[\lambda_{ds1}\lambda_{qs1}\lambda_{ds2}\lambda_{qs2}\lambda_{dr}\lambda_{qr}\right]^t \tag{1}$$

$$[V] = [V_{ds1} \quad V_{qs1} \quad V_{ds2} \quad V_{qs2} \quad 0 \quad 0]^t \tag{2}$$

$$[A] = \begin{bmatrix} 1 & 0 & 0 & 0 & 0 & 0 \\ 0 & 1 & 0 & 0 & 0 & 0 \\ 0 & 0 & 1 & 0 & 0 & 0 \\ 0 & 0 & 0 & 1 & 0 & 0 \\ 0 & 0 & 0 & 0 & 1 & 0 \\ 0 & 0 & 0 & 0 & 0 & 1 \end{bmatrix} \tag{3}$$

$$[A] = \begin{bmatrix} \frac{R_s}{\sigma}\left(1-\frac{l_s^2 L_a}{\sigma L_s^2}\right) & 0 & -\frac{R_s}{\sigma L_s}\left(l_{sm}+\frac{l_s L_a}{\sigma L_s}\right) & 0 & -\frac{R_s l_s L_a}{\sigma l_r L_s} & 0 \\ 0 & \frac{R_s}{\sigma}\left(1-\frac{l_s l_s L_a}{\sigma L_s^2}\right) & 0 & -\frac{R_s}{\sigma L_s}\left(l_{sm}+\frac{l_s L_a}{\sigma L_s}\right) & 0 & -\frac{R_{s1} l_{s2} L_a}{\sigma l_r L_{s2}} \\ \frac{R_s}{\sigma}\left(1-\frac{l_s^2 L_a}{\sigma L_s^2}\right) & 0 & -\frac{R_s}{\sigma L_s}\left(l_{sm}+\frac{l_s L_a}{\sigma L_s}\right) & 0 & -\frac{R_{s2} l_s L_a}{\sigma l_r L_s} & 0 \\ 0 & -\frac{R_s}{\sigma}\left(1-\frac{l_s^2 L_a}{\sigma L_s^2}\right) & 0 & -\frac{R_s}{\sigma L_s}\left(l_{sm}+\frac{l_s L_a}{\sigma L_s}\right) & 0 & -\frac{R_s l_s L_a}{\sigma l_r L_s} \\ -\frac{R_r L_a l_s}{\sigma L_s l_r} & 0 & -\frac{R_r L_a l_s}{\sigma L_s l_r} & 0 & \frac{R_r}{l_r}\left(1-\frac{L_a}{l_r}\right) & w_e \\ 0 & -\frac{R_r L_a l_s}{\sigma L_s l_r} & 0 & -\frac{R_r L_a l_s}{\sigma L_s l_r} & -w_e & \frac{R_r}{l_r}\left(1-\frac{L_a}{l_r}\right) \end{bmatrix}$$

with $L_s = l_s + l_{sm}$ and $\sigma = L_s - \frac{l_{sm}^2}{L_s}$ (4)

The magnetizing flux values are given by:

$$\begin{cases} \lambda_{dm} = L_a\left(\lambda_{ds1}\frac{l_s}{\sigma L_s} + \lambda_{ds2}\frac{l_s}{\sigma L_s} + \lambda_{dr}\frac{1}{l_r}\right) \\ \lambda_{qm} = L_a\left(\lambda_{qs1}\frac{l_s}{\sigma L_s} + \lambda_{qs2}\frac{l_s}{\sigma L_s} + \lambda_{qr}\frac{1}{l_r}\right) \end{cases} \tag{5}$$

where:

$$L_a = \frac{1}{\frac{1}{L_m}+\frac{2l_S}{\sigma L_S}+\frac{1}{l_r}} \tag{6}$$

Using the state variables, the following set of equations can be defined:

$$\begin{cases} i_{ds1} = \frac{1}{\sigma}\left(1-\frac{l_s^2 L_a}{\sigma L_s^2}\right)\lambda_{ds1} - \frac{1}{\sigma L_s}\left(l_{sm}+\frac{l_s L_a}{\sigma L_s}\right)\lambda_{ds2} - \left(\frac{l_s L_a}{\sigma l_r L_s}\right)\lambda_{dr} \\ i_{qs1} = \frac{1}{\sigma}\left(1-\frac{l_s^2 L_a}{\sigma L_s^2}\right)\lambda_{qs1} - \frac{1}{\sigma L_s}\left(l_{sm}+\frac{l_s L_a}{\sigma L_s}\right)\lambda_{qs2} - \left(\frac{l_s L_a}{\sigma l_r L_s}\right)\lambda_{qr} \\ i_{ds2} = \frac{1}{\sigma}\left(1-\frac{l_s^2 L_a}{\sigma L_s^2}\right)\lambda_{ds2} - \frac{1}{\sigma L_s}\left(l_{sm}+\frac{l_s L_a}{\sigma L_s}\right)\lambda_{ds1} - \left(\frac{l_s L_a}{\sigma l_r L_s}\right)\lambda_{dr} \\ i_{qs2} = \frac{1}{\sigma}\left(1-\frac{l_s^2 L_a}{\sigma L_s^2}\right)\lambda_{qs2} - \frac{1}{\sigma L_s}\left(l_{sm}+\frac{l_s L_a}{\sigma L_s}\right)\lambda_{qs1} - \left(\frac{l_s L_a}{\sigma l_r L_s}\right)\lambda_{qr} \\ i_{dr} = -\left(\frac{L_a l_s}{\sigma L_s l_r}\right)\lambda_{ds1} - \left(\frac{L_a l_s}{\sigma L_s l_r}\right)\lambda_{ds2} + \frac{1}{l_r}\left(1-\frac{L_a}{l_r}\right)\lambda_{dr} \\ i_{qr} = -\left(\frac{L_a l_s}{\sigma L_s l_r}\right)\lambda_{qs1} - \left(\frac{L_a l_s}{\sigma L_s l_r}\right)\lambda_{qs2} + \frac{1}{l_r}\left(1-\frac{L_a}{l_r}\right)\lambda_{qr} \end{cases} \tag{7}$$

III. SIMULATION AND PERFORMANCE RESULTS

To examine how the multiphase induction machine performs, both sets of the three-phase windings of the stator were connected to a variety of excitation capacitors. Figure 3 shows the diagrammatic representation of a multiphase induction machine operating in shunt mode. The test device was subjected to several conditions, including no load and loads with varying speeds and excitation capacitor values. Table I lists the generator parameters that were established by the laboratory machines' no-load and locked-rotor tests.

TABLE I. PARAMETERS OF THE GENERATOR

Sn	0.5 KW
VLL	220 V
ns	1500 rpm
I	0.75 A
f	50 Hz
Rs	28.59 Ω
Rr	14.38 Ω
Xr	19.81 Ω
Xsm	20.1 Ω
Xs	19.81 Ω

Two sets of specifically designed three-phase windings were used to rewind the stator of each machine (two stars).

A. Control Strategy of Unloaded MPIM

As no voltage is necessary for autonomous operation, the multiphase induction machine's rated voltage and current parameters listed on the equipment rating plate were used to calculate power limits, as shown in Figure 3. Voltage is sensitive to capacitance fluctuation for a specific rotational speed value. The generator starts from a minimum capacity C_{min} = 6.47μF which corresponds to a voltage V_{min} = 95V.

The machine could burn if the excitation capacity is increased because it will increase the voltage applied to the stator. Two capacity limit values were found for a given speed, one for the generator beginning and the other for the nominal voltage: $C \in [6.47, 8.19]\ \mu F$. As a result, the vacuum generator's stable operating range is limited at high rotation rates. The device starts at its rated speed *Wemin* = 279.4 rad/s, which corresponds to a voltage V = 8323 V, for a certain capacity. For a *Wemax* rated speed of 314.2 rad/s, the machine's rated voltage V = 220 V is obtained as shown in Figure 4.

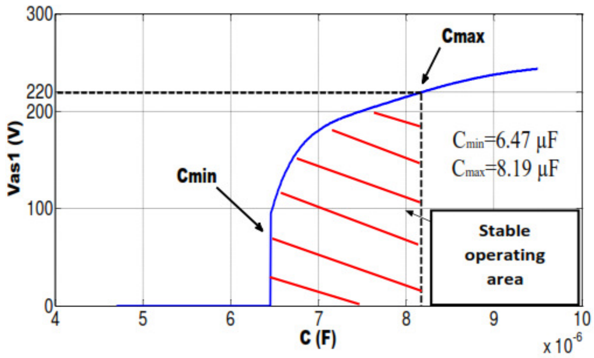

Fig. 3. Variation of voltage with capacitance.

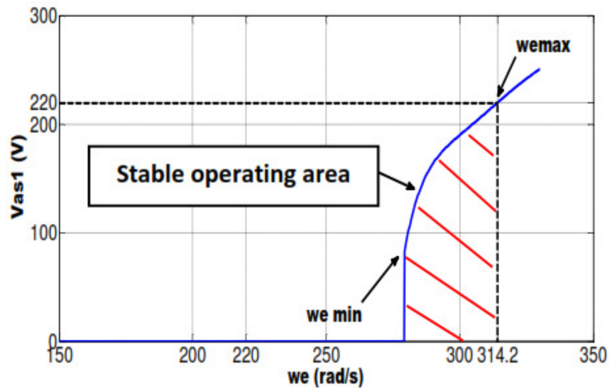

Fig. 4. Stator voltage against speed for constant capacity C= 8.19 μF.

When the speed exceeds the voltage, there is a high risk of overheating (*Wemax*) and the occurrence of damage to the machine's insulation. As a result, the speed value should be selected with care. To define the stable operating zone of the generator for self-excited induction, it is helpful to know the speed at which extreme values change, and therefore the reliable operating range of the generator is defined for a particular capacity by $\omega_{min} < \omega_e < \omega_{e\ max}$. As the excitation power rises, the stable operating range of the vacuum generator; therefore, performance at large excitation capacities is of special relevance.

B. Stability Analysis for Loaded Six-Phase Induction Generator

It can be shown that the machine's terminal voltage is more critical than the vacuum. Figure 5 shows that as the load is reduced, the voltage decreases, the current increases to its peak, and then both the voltage and the current drop to zero. *Zmax* exceeds the nominal operating conditions of the generator. As a result, *Zmin* has a minimum value below which the machine's excitement is gone. By doing this, a load range is created that guarantees that the generator will run nonstop. The selection of the load impedance must meet the following criteria:

$$Z_{min} \leq Z_{ch} \leq Z_{max} \tag{8}$$

Excitation capacity, drive speed, and load impedance affect the terminal voltage of the autonomous asynchronous generator. Figure 6 shows the performance of the machine.

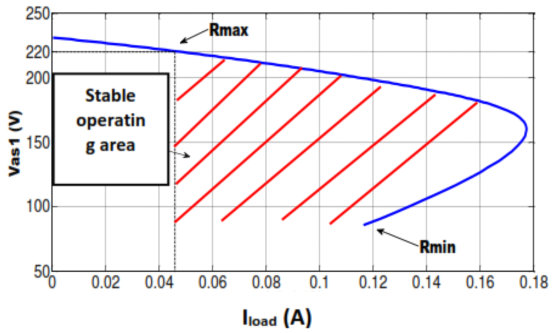

Fig. 5. Stable operating zone under load for C = 8.65 μF and we = 314.2 rad/s.

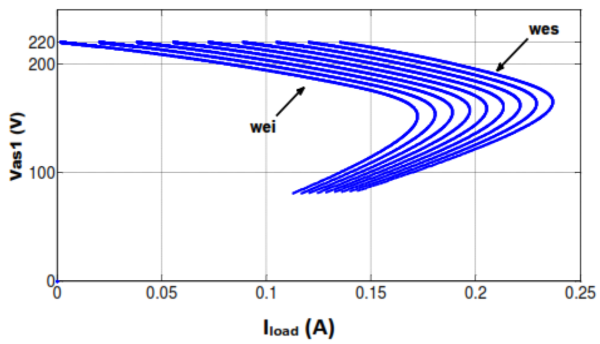

Fig. 6. Stator voltage against load current for various speeds (ω_{ei} = 300 rad/s, ω_{ef} = 316 rad/s, Δw_e = 2 rad/s, C = 9.5 μF.

TABLE II. EFFECT OF THE ROTATIONAL SPEED ON THE CRITICAL LOAD IMPEDANCE VALUES.

Speed	316 rad/s	314 rad/s	312 rad/s
Zmin	579.29Ω	592.14Ω	605.83Ω
Zmax	1626Ω	1826Ω	2097.23Ω

Table II shows that as the fixed rotational speed capacity increases, the voltage changes as a function of the load current, and the extreme values of the load impedance decrease. This reduces the variation of the load range and, as a result, the stable working range of the generator load. This creates a load range that ensures that the generator will run continuously. Impedance under maximum load decreases as the current flows are increased for a certain rotational speed. The generator's performance under load is significantly influenced by its capacitance and speed.

IV. CONCLUSIONS

Technology for multiphase machines has advanced significantly in the last ten years. This study offered a thorough analysis of a multiphase induction generator that has been successfully modeled in a fixed reference frame utilizing a different modeling strategy. The selection of the ideal excitation capacitance and some other factors, relevant to the implementation of the high-phase multiphase induction generator, were addressed in depth. The ideal excitation capacitance for the machine under investigation was determined by experimental research. The simulation findings show that the generator has excellent voltage control because of series compensation. The generating system is capable of producing output voltage at a constant frequency. Moreover, the electricity from the energy storage element can be switched to the AC side in an emergency.

ACKNOWLEDGMENT

The authors express their appreciation to the Scientific Research (DSR) at the Islamic University of Madinah for funding this research work through project number 1043.

REFERENCES

[1] H. Mellah, S. Arslan, H. Sahraoui, K. E. Hemsas, and S. Kamel, "The Effect of Stator Inter-Turn Short-Circuit Fault on DFIG Performance Using FEM," *Engineering, Technology & Applied Science Research*, vol. 12, no. 3, pp. 8688–8693, Jun. 2022, https://doi.org/10.48084/etasr.4923.

[2] A. Guediri, "Study and Order of a Medium Power Wind Turbine Conversion Chain Connected to Medium Voltage Grid," *Engineering, Technology & Applied Science Research*, vol. 11, no. 3, pp. 7279–7282, Jun. 2021, https://doi.org/10.48084/etasr.4169.

[3] H. H. Bui, "Control Design for the Ward–Leonard System in Wind Turbines," *Engineering, Technology & Applied Science Research*, vol. 13, no. 1, pp. 9968–9972, Feb. 2023, https://doi.org/10.48084/etasr.5425.

[4] M. A. Khlifi and M. B. Slimene, "Efficiency of a Six-Phase Induction Generator Employing a Static Excitation Controller to Generate AC Power for Wind Energy," *IEEE Access*, vol. 11, pp. 28791–28799, 2023, https://doi.org/10.1109/ACCESS.2023.3260775.

[5] M. Ben Slimene and M. A. Khlifi, "Investigation on the Effects of Magnetic Saturation in Six-Phase Induction Machines with and without Cross Saturation of the Main Flux Path," *Energies*, vol. 15, no. 24, Jan. 2022, Art. no. 9412, https://doi.org/10.3390/en15249412.

[6] H. P. Nabi, P. Dadashi, and A. Shoulaie, "A novel structure for vector control of a symmetrical six-phase induction machine with three current sensors," in *2011 10th International Conference on Environment and Electrical Engineering*, Rome, Italy, Feb. 2011, pp. 1–5, https://doi.org/10.1109/EEEIC.2011.5874735.

[7] M. A. Khlifi, "Explaining the d-q Magnetic Couplings Theoretically in Saturated Smooth Air-Gap AC Machines," *Engineering, Technology & Applied Science Research*, vol. 9, no. 1, pp. 3739–3743, Feb. 2019, https://doi.org/10.48084/etasr.2327.

[8] I. Sami, S. Ullah, Z. Ali, N. Ullah, and J.-S. Ro, "A Super Twisting Fractional Order Terminal Sliding Mode Control for DFIG-Based Wind Energy Conversion System," *Energies*, vol. 13, no. 9, Jan. 2020, Art. no. 2158, https://doi.org/10.3390/en13092158.

[9] M. M. Alhato, M. N. Ibrahim, H. Rezk, and S. Bouallègue, "An Enhanced DC-Link Voltage Response for Wind-Driven Doubly Fed Induction Generator Using Adaptive Fuzzy Extended State Observer and Sliding Mode Control," *Mathematics*, vol. 9, no. 9, Jan. 2021, Art. no. 963, https://doi.org/10.3390/math9090963.

[10] H. Benbouhenni, Z. Boudjema, and A. Belaidi, "DPC Based on ANFIS Super-Twisting Sliding Mode Algorithm of a Doubly-Fed Induction Generator for Wind Energy System," *Journal Européen des Systèmes Automatisés*, vol. 53, no. 1, pp. 69–80, Feb. 2020, https://doi.org/10.18280/jesa.530109.

[11] B. Farid, B. Tarek, and B. Sebti, "Fuzzy super twisting algorithm dual direct torque control of doubly fed induction machine," *International Journal of Electrical and Computer Engineering (IJECE)*, vol. 11, no. 5, Oct. 2021, Art. no. 3782, https://doi.org/10.11591/ijece.v11i5.pp3782-3790.

[12] N. Ullah, I. Sami, Md. S. Chowdhury, K. Techato, and H. I. Alkhammash, "Artificial Intelligence Integrated Fractional Order Control of Doubly Fed Induction Generator-Based Wind Energy

System," *IEEE Access*, vol. 9, pp. 5734–5748, 2021, https://doi.org/10.1109/ACCESS.2020.3048420.

[13] A. Guediri and S. Touil, "Modeling and Comparison of Fuzzy-PI and Genetic Control Algorithms for Active and Reactive Power Flow between the Stator (DFIG) and the Grid," *Engineering, Technology & Applied Science Research*, vol. 12, no. 3, pp. 8640–8645, Jun. 2022, https://doi.org/10.48084/etasr.4905.

[14] F. Bu, Y. Hu, W. Huang, S. Zhuang, and K. Shi, "Wide-Speed-Range-Operation Dual Stator-Winding Induction Generator DC Generating System for Wind Power Applications," *IEEE Transactions on Power Electronics*, vol. 30, no. 2, pp. 561–573, Oct. 2015, https://doi.org/10.1109/TPEL.2014.2308222.

[15] M. B. Slimene and M. A. Khlifi, "Performance Limits of Three-Phase Self-Excited Induction Generator (SEIG) as a Stand Alone DER," *Journal of Electrical Engineering & Technology*, vol. 12, no. 1, pp. 145–150, Jan. 2017.

[16] M. A. Khlifi and H. Rehaoulia, "General modeling of saturated AC machines for industrial drives," *COMPEL: The International Journal for Computation and Mathematics in Electrical and Electronic Engineering*, vol. 35, no. 1, pp. 44–63, Jan. 2016, https://doi.org/10.1108/COMPEL-12-2014-0346.

[17] M. A. Taghikhani and A. D. Farahani, "A Reactive Power Based Reference Model for Adaptive Control Strategy in a SEIG," *Engineering, Technology & Applied Science Research*, vol. 8, no. 1, pp. 2477–2484, Feb. 2018, https://doi.org/10.48084/etasr.1701.

[18] M. B. Slimene, M. A. Khlifi, M. B. Fredj, and H. Rehaoulia, "Modeling of a Dual Stator Induction Generator with and Without Cross Magnetic Saturation," *Journal of Magnetics*, vol. 20, no. 3, pp. 284–289, Sep. 2015.

[19] M. Ben Slimene, M. A. Khlifi, M. Ben Fredj, and H. Rehaoulia, "Analysis of Saturated Self-Excited Dual Stator Induction Generator for Wind Energy Generation," *Journal of Circuits, Systems and Computers*, vol. 24, no. 09, Art. no. 1550129, Oct. 2015, https://doi.org/10.1142/S0218126615501297.

[20] M. A. Khlifi and B. M. Alshammari, "Steady State Analysis of an Isolated Self-Excited Dual Three-Phase Induction Generator for Renewable Energy," *International Journal of Modern Nonlinear Theory and Application*, vol. 03, no. 05, Nov. 2014, Art. no. 191, https://doi.org/10.4236/ijmnta.2014.35021.

[21] B. S. Marwa, A. K. Mohamed, B. F. Mouldi, and R. Habib, "Effect of the stator mutual leakage reactance of dual stator induction generator," *International Journal of Electrical Energy*, vol. 2, no. 3, pp. 1810–1818, 2014.

[22] M. B. Slimene, M. A. Khlifi, M. Benfredj, and H. Rehaoulia, "The Process of Self Excitation in Dual Three-Phase Induction Generator," *International Review of Electrical Engineering*, vol. 8, no. 6, pp. 1738–1743, Dec. 2013.

[23] M. A. Khlifi, M. Ben Slimene, M. Ben Fredj, and H. Rhaoulia, "Performance evaluation of self-excited DSIG as a stand-alone distributed energy resources," *Electrical Engineering*, vol. 98, no. 2, pp. 159–167, Jun. 2016, https://doi.org/10.1007/s00202-015-0349-y.

[24] M. Slunjski, O. Dordevic, M. Jones, and E. Levi, "Symmetrical/Asymmetrical Winding Reconfiguration in Multiphase Machines," *IEEE Access*, vol. 8, pp. 12835–12844, 2020, https://doi.org/10.1109/ACCESS.2020.2965652.

[25] J. Paredes, B. Prieto, M. Satrústegui, I. Elósegui, and P. González, "Improving the Performance of a 1-MW Induction Machine by Optimally Shifting From a Three-Phase to a Six-Phase Machine Design by Rearranging the Coil Connections," *IEEE Transactions on Industrial Electronics*, vol. 68, no. 2, pp. 1035–1045, Oct. 2021, https://doi.org/10.1109/TIE.2020.2969099.

[26] Y. Wang, J. Yang, R. Deng, and G. Yang, "Parameters estimation for multiphase induction machine with concentrated windings through finite element method," *IET Electric Power Applications*, vol. 14, no. 10, pp. 1807–1817, 2020, https://doi.org/10.1049/iet-epa.2019.0869.

[27] T. S. de Souza, R. R. Bastos, and B. J. Cardoso Filho, "Synchronous-Frame Modeling and dq Current Control of an Unbalanced Nine-Phase Induction Motor Due to Open Phases," *IEEE Transactions on Industry Applications*, vol. 56, no. 2, pp. 2097–2106, Mar. 2020, https://doi.org/10.1109/TIA.2020.2965493.

[28] P. Drozdowski and D. Cholewa, "Voltage Control of Multiphase Cage Induction Generators at a Speed Varying over a Wide Range," *Energies*, vol. 14, no. 21, Art. no. 7080, Jan. 2021, https://doi.org/10.3390/en14217080.

[29] M. F. Khan and M. R. Khan, "Modeling and Analysis of a Six-Phase Self Excited Induction Generator Feeding Induction Motors," *IEEE Transactions on Energy Conversion*, vol. 36, no. 2, pp. 746–754, Jun. 2021, https://doi.org/10.1109/TEC.2020.3013784.

[30] A. Gonzalez-Prieto, I. González-Prieto, M. J. Duran, and J. J. Aciego, "Dynamic Response in Multiphase Electric Drives: Control Performance and Influencing Factors," *Machines*, vol. 10, no. 10, Oct. 2022, Art. no. 866, https://doi.org/10.3390/machines10100866.

[31] M. R. Arahal, M. G. Satué, F. Barrero, and C. Martín, "Online Adaptive Set of Virtual Voltage Vectors for Stator Current Regulation of a Six-Phase Induction Machine Using Finite State Model Predictive Controllers," *Applied Sciences*, vol. 13, no. 7, Jan. 2023, Art. no. 4113, https://doi.org/10.3390/app13074113.

[32] L. Li, W. Zhou, X. Bi, X. Sun, and X. Shi, "Second-Order Model-Based Predictive Control of Dual Three-Phase PMSM Based on Current Loop Operation Optimization," *Actuators*, vol. 11, no. 9, Sep. 2022, Art. no. 251, https://doi.org/10.3390/act11090251.

[33] W. Taha, P. Azer, A. D. Callegaro, and A. Emadi, "Multiphase Traction Inverters: State-of-the-Art Review and Future Trends," *IEEE Access*, vol. 10, pp. 4580–4599, 2022, https://doi.org/10.1109/ACCESS.2022.3141542.

[34] K. B. Tawfiq, M. N. Ibrahim, E. E. EL-Kholy, and P. Sergeant, "Performance Analysis of a Rewound Multiphase Synchronous Reluctance Machine," *IEEE Journal of Emerging and Selected Topics in Power Electronics*, vol. 10, no. 1, pp. 297–309, Oct. 2022, https://doi.org/10.1109/JESTPE.2021.3106591.